


Revisiting the transition $\Xi_{cc}^{++} \rightarrow \Xi_c^{(\prime)+}$ to understand the data from LHCb

Hong-Wei Ke^{1,*} and Xue-Qian Li^{2,†}

¹*School of Science, Tianjin University, Tianjin 300072, China*

²*School of Physics, Nankai University, Tianjin 300071, China*

 (Received 27 March 2022; accepted 25 April 2022; published 13 May 2022)

The LHCb collaboration newly measured the decay rate of doubly charmed baryon $\Xi_{cc}^{++} \rightarrow \Xi^{\prime+} \pi^+$, and a ratio of its branching fraction with respect to that of the decay $\Xi_{cc}^{++} \rightarrow \Xi^+ \pi^+$ is reported as $1.41 \pm 0.17 \pm 0.10$. This result conflicts with the theoretical predictions made by several groups. In our previous work, following the prescription given in early literature where the us diquark in Ξ_c^+ is assumed to be a scalar, whereas in $\Xi_c^{\prime+}$ it is a vector, i.e., the spin-flavor structure of Ξ_c^+ is $[us]_0 c$ and that of $\Xi_c^{\prime+}$ is $[us]_1 c$, we studied the case of $\Xi_{cc}^{++} \rightarrow \Xi^{(\prime)+}$ with the light-front quark model. Numerically we obtained $\Gamma(\Xi_{cc}^{++} \rightarrow \Xi^{\prime+} \pi^+)/\Gamma(\Xi_{cc}^{++} \rightarrow \Xi^+ \pi^+) = 0.56 \pm 0.18$, which is about half of the data. While abandoning the presupposition, we suppose the spin-flavor structure of $[us]c$ in Ξ_c^+ may be a mixture of $[us]_0 c$ and $[us]_1 c$, namely the spin-flavor function of Ξ_c^+ could be $\cos \theta [us]_0 [c] + \sin \theta [us]_1 [c]$. An alternative combination $-\sin \theta [us]_0 [c] + \cos \theta [us]_1 [c]$ would correspond to $\Xi_c^{\prime+}$. Introducing the mixing mechanism, the ratio $\Gamma(\Xi_{cc}^{++} \rightarrow \Xi^{\prime+} \pi^+)/\Gamma(\Xi_{cc}^{++} \rightarrow \Xi^+ \pi^+)$ depends on the mixing angle θ . With the mixing scenario, the theoretical prediction on the ratio between the transition rate of $\Xi_{cc}^{++} \rightarrow \Xi_c^{\prime+}$ and that of $\Xi_{cc}^{++} \rightarrow \Xi_c^+$ can coincide with the data as long as $\theta = 16.27^\circ \pm 2.30^\circ$ or $85.54^\circ \pm 2.30^\circ$ is set. Definitely, more precise measurements on other decay portals of Ξ_{cc}^{++} are badly needed for testing the mixing mechanism and further determining the mixing angle.

DOI: 10.1103/PhysRevD.105.096011

I. INTRODUCTION

In 2017, the LHCb collaboration observed the doubly charmed baryon Ξ_{cc}^{++} [1] in the four-body final state $\Lambda_c K^- \pi^+ \pi^+$ [1] and the $\Xi^+ \pi^+$ portals [2] successively. That baryon was expected for a long time by physicists of high-energy physics because of its significance. The quark model predicted existence of baryons with two or three heavy quarks but they had evaded experimental observation for long. With the great progress of detecting facilities and techniques, recently the LHCb collaboration observed the doubly charmed baryon via a decay portal $\Xi_{cc}^{++} \rightarrow \Xi^{\prime+} \pi^+$, with a branching fraction relative to that of the decay $\Xi_{cc}^{++} \rightarrow \Xi^+ \pi^+$ being $1.41 \pm 0.17 \pm 0.10$ [3].

On the theoretical aspect, some approaches have been applied to study the weak decay $\Xi_{cc}^{++} \rightarrow \Xi^{(\prime)+}$. In Refs. [4–12] the predicted ratio $\Gamma(\Xi_{cc}^{++} \rightarrow \Xi^{\prime+} \pi^+)/\Gamma(\Xi_{cc}^{++} \rightarrow \Xi^+ \pi^+)$ was not in keeping with the data. In our earlier work [13] the transition $\Xi_{cc}^{++} \rightarrow \Xi^{(\prime)+}$ was explored within the light-front

quark model [14–38], where the three-quark picture of baryon was adopted. In that approach one needs to determine the vertex functions for the baryons by means of their inner structures. For Ξ_{cc}^{++} a naive and reasonable conjecture suggests that the two c quarks compose a physical subsystem (or a diquark) which serves as a color source for the light quark [39,40]. The relative orbital angular momentum between the two c quarks is 0, i.e., the cc pair is in an S wave, and because it is in a color-antitriplet $\bar{3}$, the spin of the cc pair must be 1 due to the symmetry requirement. In the works about single-charmed baryons, usually the two light quarks are supposed to reside in a subsystem as the light diquark [41,42]. In that literature, a presupposition Ref. [42] suggests that the us diquark in Ξ_c^+ is a scalar, whereas it is a vector in $\Xi_c^{\prime+}$.

In the transition $\Xi_{cc}^{++} \rightarrow \Xi^{(\prime)+}$ one c quark in the initial state would decay into an s quark via weak interaction while the other c quark and u quark are spectators in the process but the cu pair is not a diquark (or a physical subsystem) in the initial state, neither in the final state. To utilize the spectator scenario, the quark structure of $[cc]_1 u$ ($[us]_0 c$ or $[us]_1 c$) should be mathematically rearranged into a sum of $\sum_i c [cu]_i$ ($\sum_i s [cu]_i$) where the sum runs over all possible spin projections via a Racah transformation. It is found that the spectator cu is independent of the quark (c or s) which is involved in the transition process. Thus the

*khw020056@tju.edu.cn

†lixq@nankai.edu.cn

Published by the American Physical Society under the terms of the [Creative Commons Attribution 4.0 International license](https://creativecommons.org/licenses/by/4.0/). Further distribution of this work must maintain attribution to the author(s) and the published article's title, journal citation, and DOI. Funded by SCOAP³.

transition process can be divided into two steps: First, the physical structure $[cc]_1u$ is rearranged into $[cu]_i c$ by a Racah transformation and then the single c quark decays into s by emitting a gauge boson while the subsystem of $[cu]_i$ remains unchanged; second, the $[cu]_i s$ structure in the final state is reordered into the $[us]_0 c$ or $[us]_1 c$ structure through another Racah transformation. In our earlier work on the transition $\Xi_{cc}^{++} \rightarrow \Xi^{(\prime)+}$ [13] the three quarks are treated as individual subjects, i.e., possess their own momenta, and we obtained the branching ratio $\Gamma(\Xi_{cc}^{++} \rightarrow \Xi^{\prime+}\pi^+)/\Gamma(\Xi_{cc}^{++} \rightarrow \Xi^+\pi^+)$ as 0.56 ± 0.18 , which is almost half of the data.

It is noted that the earlier calculation in [13] was based on the presupposition that the us diquark in Ξ_c^+ is a scalar whereas that in $\Xi_c^{\prime+}$ is a vector [42]. As is well known, the flavor symmetry is broken so either the $[us]c$ spin-flavor structure in Ξ_c^+ or in $\Xi_c^{\prime+}$ could be a mixture of $[us]_0 c$ and $[us]_1 c$. In this new scenario a mixing angle θ ($0 < \theta < \pi$) should be introduced for the mixing of flavor-spin wave functions, i.e., $\Xi_c^+ = \cos\theta[us]_0[c] + \sin\theta[us]_1[c]$ and $\Xi_c^{\prime+} = -\sin\theta[us]_0[c] + \cos\theta[us]_1[c]$, where the subscript 0 or 1 represents the total spin of the us subsystem. When θ is set to 0, i.e., $\Xi_c^+ = [us]_0[c]$ and $\Xi_c^{\prime+} = [us]_1[c]$, the structures of Ξ_c^+ and $\Xi_c^{\prime+}$ restore the original setting supposed by the authors of Ref. [42]. In other words the transition matrix elements $\mathcal{A}(\Xi_{cc}^{++} \rightarrow \Xi_c^+)$ and $\mathcal{A}(\Xi_{cc}^{++} \rightarrow \Xi_c^{\prime+})$ carried out in Ref. [13] just correspond to the processes $\mathcal{A}([cc]_1[u] \rightarrow [us]_0[c])$ and $\mathcal{A}([cc]_1[u] \rightarrow [us]_1[c])$. Now, as long as θ is not equal to 0, the process for $\mathcal{A}(\Xi_{cc}^{++} \rightarrow \Xi_c^+)$ should be replaced by $\cos\theta\mathcal{A}([cc]_1[u] \rightarrow [us]_0[c]) + \sin\theta\mathcal{A}([cc]_1[u] \rightarrow [us]_1[c])$, while for $\mathcal{A}(\Xi_{cc}^{++} \rightarrow \Xi_c^{\prime+})$ the process is $-\sin\theta\mathcal{A}([cc]_1[u] \rightarrow [us]_0[c]) + \cos\theta\mathcal{A}([cc]_1[u] \rightarrow [us]_1[c])$. The simple extension means existence of new subtransition matrix elements for $\Xi_{cc}^{++} \rightarrow \Xi_c^+$ and $\Xi_{cc}^{++} \rightarrow \Xi_c^{\prime+}$. The mixture scenario changes the predicted rate from the old picture; obviously, the newly obtained theoretical estimate on the rates depend on θ .

This paper is organized as follows: after the Introduction, in Sec. II we revisit the transition matrix element for $\Xi_{cc}^{++} \rightarrow \Xi_c^{(\prime)+}$ in the light-front quark model. Our numerical results for $\Xi_{cc}^{++} \rightarrow \Xi_c^{(\prime)+}$ are presented in Sec. III. Section IV is devoted to our conclusion and discussions.

II. $\Xi_{cc}^{++} \rightarrow \Xi_c^{(\prime)+}$ IN THE LIGHT-FRONT QUARK MODEL

A. The structures of Ξ_{cc}^{++} , Ξ_c^+ , and $\Xi_c^{\prime+}$

The spectator scenario may greatly alleviate the theoretical difficulties for calculating the hadronic transition matrix elements. However, the diquarks (physical subsystems) cc and us in Ξ_{cc}^{++} and $\Xi_c^{(\prime)+}$ are not spectators, which means the spectator approximation cannot be directly applied. In fact, the c and u quarks which do not undergo a transition in the process, i.e., the combination

of cu , are approximately regarded as a spectator (an effective subsystem).

As a three-body system, the total spin of a baryon can be realized by different constructing schemes and the Racah transformations can relate one to others. By the aforementioned rearrangement of quark flavors the physical states $[cc]_1u$ and $[us]_0c$ (or $[us]_1c$) are written into sums over the effective forms $c[cu]_i$ and $s[cu]_i$, respectively. The detailed transformations are [4]

$$[c^1 c^2]_1[u] = \frac{\sqrt{2}}{2} \left(-\frac{\sqrt{3}}{2} [c^2][c^1 u]_0 + \frac{1}{2} [c^2][c^1 u]_1 - \frac{\sqrt{3}}{2} [c^1][c^2 u]_0 + \frac{1}{2} [c^1][c^2 u]_1 \right), \quad (1)$$

$$[us]_0[c] = -\frac{1}{2} [s][cu]_0 + \frac{\sqrt{3}}{2} [s][cu]_1, \quad (2)$$

$$[us]_1[c] = \frac{\sqrt{3}}{2} [s][cu]_0 + \frac{1}{2} [s][cu]_1. \quad (3)$$

In Ref. [42] $\Xi_{cc}^{++} \equiv [c^1 c^2]_1[u]$, $\Xi_c^+ \equiv [us]_0[c]$, and $\Xi_c^{\prime+} \equiv [us]_1[c]$. Instead, in this work we suppose Ξ_c^+ and $\Xi_c^{\prime+}$ to be mixtures of $[us]_0[c]$ and $[us]_1[c]$, i.e., $\Xi_c^+ = \cos\theta[us]_0[c] + \sin\theta[us]_1[c]$ and $\Xi_c^{\prime+} = -\sin\theta[us]_0[c] + \cos\theta[us]_1[c]$, where θ is the mixing angle (restricted in the first and second quadrants with $0 < \theta < \pi$).

B. The form factors of $\Xi_{cc}^{++} \rightarrow \Xi_c^+$ and $\Xi_{cc}^{++} \rightarrow \Xi_c^{\prime+}$ in LFQM

The leading Feynman diagram responsible for the weak decay $\Xi_{cc}^{++} \rightarrow \Xi_c^{(\prime)+}$ is shown in Fig. 1. Following the procedures given in Refs. [32–35] the transition matrix element can be computed with the vertex functions of

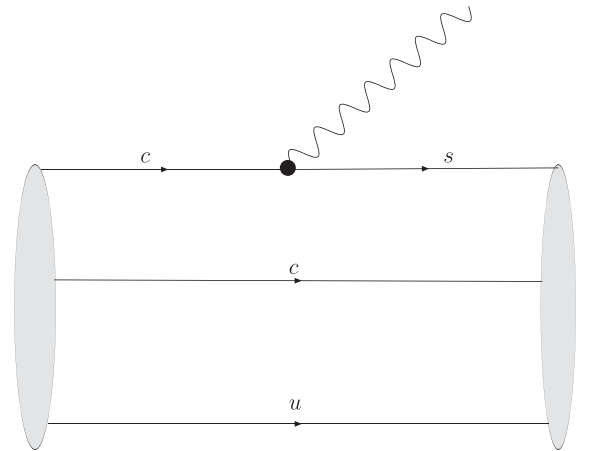


FIG. 1. The Feynman diagrams for $\Xi_{cc}^{++} \rightarrow \Xi_c^{(\prime)+}$ transitions, where \bullet denotes $V - A$ current vertex.

$|\Xi_{cc}^{++}(P, S, S_z)\rangle$ and $|\Xi_c^{(+)}(P', S', S'_z)\rangle$. The cu subsystem stands as a spectator, i.e., its spin configuration does not change during the transition.

The form factors for the weak transition $\Xi_{cc}^{++} \rightarrow \Xi_c^+$ are defined in the standard way as

$$\begin{aligned} \langle \Xi_c^+(P', S', S'_z) | \bar{s} \gamma_\mu (1 - \gamma_5) c | \Xi_{cc}^{++}(P, S, S_z) \rangle &= \bar{u}_{\Xi_c^+}(P', S'_z) \left[\gamma_\mu f_1(q^2) + i \sigma_{\mu\nu} \frac{q^\nu}{M_{\Xi_{cc}^{++}}} f_2(q^2) + \frac{q_\mu}{M_{\Xi_{cc}^{++}}} f_3(q^2) \right] u_{\Xi_{cc}^{++}}(P, S_z) \\ &\quad - \bar{u}_{\Xi_c^+}(P', S'_z) \left[\gamma_\mu g_1(q^2) + i \sigma_{\mu\nu} \frac{q^\nu}{M_{\Xi_c^+}} g_2(q^2) + \frac{q_\mu}{M_{\Xi_{cc}^{++}}} g_3(q^2) \right] \gamma_5 u_{\Xi_{cc}^{++}}(P, S_z), \end{aligned} \quad (4)$$

where $q \equiv P - P'$. In terms of the spin-flavor structures of Ξ_{cc}^{++} and Ξ_c^+ the matrix element $\langle \Xi_c^+(P', S', S'_z) | \bar{s} \gamma_\mu (1 - \gamma_5) c | \Xi_{cc}^{++}(P, S, S_z) \rangle$ can be written as

$$\cos \theta \langle [s][cu]_0 | \bar{s} \gamma_\mu (1 - \gamma_5) c | [c][cu]_0 \rangle + \sin \theta \langle [s][cu]_1 | \bar{s} \gamma_\mu (1 - \gamma_5) c | [c][cu]_1 \rangle.$$

For the transition matrix elements $\langle [s][cu]_0 | \bar{s} \gamma_\mu (1 - \gamma_5) c | [c][cu]_0 \rangle$ and $\langle [s][cu]_1 | \bar{s} \gamma_\mu (1 - \gamma_5) c | [c][cu]_1 \rangle$ the form factors are denoted to f_i^s, g_i^s and f_i^v, g_i^v , so we have

$$\begin{aligned} f_1 &= \left(\frac{\sqrt{6}}{4} \cos \theta - \frac{3\sqrt{2}}{4} \sin \theta \right) f_1^s + \left(\frac{\sqrt{6}}{4} \cos \theta + \frac{\sqrt{2}}{4} \sin \theta \right) f_1^v, \\ g_1 &= \left(\frac{\sqrt{6}}{4} \cos \theta - \frac{3\sqrt{2}}{4} \sin \theta \right) g_1^s + \left(\frac{\sqrt{6}}{4} \cos \theta + \frac{\sqrt{2}}{4} \sin \theta \right) g_1^v, \\ f_2 &= \left(\frac{\sqrt{6}}{4} \cos \theta - \frac{3\sqrt{2}}{4} \sin \theta \right) f_2^s + \left(\frac{\sqrt{6}}{4} \cos \theta + \frac{\sqrt{2}}{4} \sin \theta \right) f_2^v, \\ g_2 &= \left(\frac{\sqrt{6}}{4} \cos \theta - \frac{3\sqrt{2}}{4} \sin \theta \right) g_2^s + \left(\frac{\sqrt{6}}{4} \cos \theta + \frac{\sqrt{2}}{4} \sin \theta \right) g_2^v, \end{aligned} \quad (5)$$

and $f_i^s, g_i^s, f_i^v, g_i^v$ can be found in our earlier paper [29].

For the transition $\langle \Xi_c^{'+}(P', S', S'_z) | \bar{s} \gamma_\mu (1 - \gamma_5) c | \Xi_{cc}^{++}(P, S, S_z) \rangle$ the form factors are also defined as done in Eq. (4). Here we just add a symbol “'” on $f_1, f_2, g_1,$ and g_2 to distinguish the quantities for $\Xi_{cc}^{++} \rightarrow \Xi_c^+$ and those for $\Xi_{cc}^{++} \rightarrow \Xi_c^{'+}$. They are

$$\begin{aligned} f'_1 &= \left(-\frac{\sqrt{6}}{4} \sin \theta - \frac{3\sqrt{2}}{4} \cos \theta \right) f_1^s + \left(-\frac{\sqrt{6}}{4} \sin \theta + \frac{\sqrt{2}}{4} \cos \theta \right) f_1^v, \\ g'_1 &= \left(-\frac{\sqrt{6}}{4} \sin \theta - \frac{3\sqrt{2}}{4} \cos \theta \right) g_1^s + \left(-\frac{\sqrt{6}}{4} \sin \theta + \frac{\sqrt{2}}{4} \cos \theta \right) g_1^v, \\ f'_2 &= \left(-\frac{\sqrt{6}}{4} \sin \theta - \frac{3\sqrt{2}}{4} \cos \theta \right) f_2^s + \left(-\frac{\sqrt{6}}{4} \sin \theta + \frac{\sqrt{2}}{4} \cos \theta \right) f_2^v, \\ g'_2 &= \left(-\frac{\sqrt{6}}{4} \sin \theta - \frac{3\sqrt{2}}{4} \cos \theta \right) g_2^s + \left(-\frac{\sqrt{6}}{4} \sin \theta + \frac{\sqrt{2}}{4} \cos \theta \right) g_2^v. \end{aligned} \quad (6)$$

III. NUMERICAL RESULTS

A. The form factors for $\Xi_{cc}^{++} \rightarrow \Xi_c^+$ and $\Xi_{cc}^{++} \rightarrow \Xi_c^{'+}$

In Ref. [13] we used a polynomial to parametrize these form factors $f_i^s, g_i^s, f_i^v,$ and g_i^v ($i = 1, 2$),

$$F(q^2) = F(0) \left[1 + a \left(\frac{q^2}{M_{\Xi_{cc}^{++}}^2} \right) + b \left(\frac{q^2}{M_{\Xi_{cc}^{++}}^2} \right)^2 + c \left(\frac{q^2}{M_{\Xi_{cc}^{++}}^2} \right)^3 \right]. \quad (7)$$

TABLE I. The form factors given in polynomial form.

F	$F(0)$	a	b	c
f_1^s	0.586	1.57	1.59	0.704
f_2^s	-0.484	2.06	2.42	1.17
g_1^s	0.420	0.983	0.692	0.258
g_2^s	0.228	1.90	2.07	0.960
f_1^v	0.610	2.04	2.27	1.06
f_2^v	0.463	2.14	2.49	1.19
g_1^v	-0.140	0.422	0.0931	0.00632
g_2^v	0.0673	0.925	0.245	-0.0862

The fitted values of a , b , c , and $F(0)$ in the form factors are presented in Table I. With the form factors, we reestimate the decay rates of semileptonic and nonleptonic decays with the new scenario for the diquark structures.

B. Nonleptonic decays of $\Xi_{cc}^{++} \rightarrow \Xi_c^+ + M$ and $\Xi_{cc}^{++} \rightarrow \Xi_c'^+ + M$

The transition matrix element of the nonleptonic decay is complicated due to involving nonperturbative physics. We did the calculation in Ref. [13] by employing the factorization assumption,

$$\begin{aligned} & \langle \Xi_c^{(\prime)+}(P', S'_z) M | \mathcal{H} | \Xi_{cc}^{++}(P, S_z) \rangle \\ &= \frac{G_F V_{cs} V_{qq'}^*}{\sqrt{2}} f_M \langle \Xi_c^{(\prime)+}(P', S'_z) | \bar{s} \gamma^\mu (1 - \gamma_5) c | \Xi_{cc}^{++}(P, S_z) \rangle, \end{aligned} \quad (8)$$

TABLE II. The widths (in unit 10^{10} s^{-1}) and up-down asymmetry of nonleptonic decays $\Xi_{cc}^{++} \rightarrow \Xi_c^{(\prime)+} M$ in [13] ($\theta = 0^\circ$).

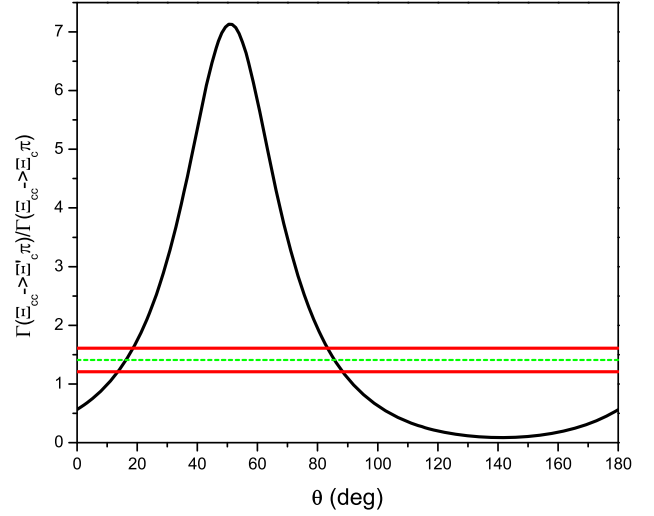
Mode	Width	Up-down asymmetry	Mode	Width	Up-down asymmetry
$\Xi_{cc}^{++} \rightarrow \Xi_c^+ \pi$	13.6 ± 1.8	-0.441 ± 0.009	$\Xi_{cc}^{++} \rightarrow \Xi_c'^+ \pi$	7.68 ± 0.92	-0.982 ± 0.005
$\Xi_{cc}^{++} \rightarrow \Xi_c^+ \rho$	11.0 ± 1.5	-0.429 ± 0.016	$\Xi_{cc}^{++} \rightarrow \Xi_c'^+ \rho$	13.9 ± 1.2	-0.111 ± 0.034
$\Xi_{cc}^{++} \rightarrow \Xi_c^+ K$	1.03 ± 0.14	-0.402 ± 0.008	$\Xi_{cc}^{++} \rightarrow \Xi_c'^+ K$	0.492 ± 0.059	-0.998 ± 0.002
$\Xi_{cc}^{++} \rightarrow \Xi_c^+ K^*$	0.414 ± 0.055	-0.422 ± 0.021	$\Xi_{cc}^{++} \rightarrow \Xi_c'^+ K^*$	0.623 ± 0.052	-0.014 ± 0.030

TABLE III. The widths (in unit 10^{10} s^{-1}) and up-down asymmetry of nonleptonic decays $\Xi_{cc}^{++} \rightarrow \Xi_c^{(\prime)+} M$ with $\theta = 16.27^\circ \pm 2.30^\circ$.

Mode	Width	Up-down asymmetry	Mode	Width	Up-down asymmetry
$\Xi_{cc}^{++} \rightarrow \Xi_c^+ \pi$	8.37 ± 0.69	-0.087 ± 0.070	$\Xi_{cc}^{++} \rightarrow \Xi_c'^+ \pi$	11.8 ± 0.5	-0.991 ± 0.006
$\Xi_{cc}^{++} \rightarrow \Xi_c^+ \rho$	5.59 ± 0.56	-0.167 ± 0.079	$\Xi_{cc}^{++} \rightarrow \Xi_c'^+ \rho$	17.6 ± 0.3	-0.228 ± 0.014
$\Xi_{cc}^{++} \rightarrow \Xi_c^+ K$	0.642 ± 0.052	-0.081 ± 0.063	$\Xi_{cc}^{++} \rightarrow \Xi_c'^+ K$	0.789 ± 0.041	-0.967 ± 0.010
$\Xi_{cc}^{++} \rightarrow \Xi_c^+ K^*$	0.187 ± 0.021	-0.211 ± 0.084	$\Xi_{cc}^{++} \rightarrow \Xi_c'^+ K^*$	0.756 ± 0.011	-0.107 ± 0.011

TABLE IV. The widths (in unit 10^{10} s^{-1}) and up-down asymmetry of nonleptonic decays $\Xi_{cc}^{++} \rightarrow \Xi_c^{(\prime)+} M$ with $\theta = 85.54^\circ \pm 2.30^\circ$.

Mode	Width	Up-down asymmetry	Mode	Width	Up-down asymmetry
$\Xi_{cc}^{++} \rightarrow \Xi_c^+ \pi$	8.36 ± 0.69	-0.952 ± 0.023	$\Xi_{cc}^{++} \rightarrow \Xi_c'^+ \pi$	11.8 ± 0.6	-0.507 ± 0.032
$\Xi_{cc}^{++} \rightarrow \Xi_c^+ \rho$	16.8 ± 0.9	-0.106 ± 0.023	$\Xi_{cc}^{++} \rightarrow \Xi_c'^+ \rho$	8.23 ± 0.67	-0.456 ± 0.004
$\Xi_{cc}^{++} \rightarrow \Xi_c^+ K$	0.554 ± 0.049	-0.977 ± 0.039	$\Xi_{cc}^{++} \rightarrow \Xi_c'^+ K$	0.869 ± 0.038	-0.455 ± 0.029
$\Xi_{cc}^{++} \rightarrow \Xi_c^+ K^*$	0.834 ± 0.042	-0.005 ± 0.013	$\Xi_{cc}^{++} \rightarrow \Xi_c'^+ K^*$	0.269 ± 0.027	-0.419 ± 0.008

FIG. 2. The dependence of $\Gamma(\Xi_{cc}^{++} \rightarrow \Xi_c^+ \pi) / \Gamma(\Xi_{cc}^{++} \rightarrow \Xi_c'^+ \pi)$ on θ .

where f_M is the decay constant of meson M . Besides the decay rate, the up-down asymmetry parameter α (its definition can be found in the Appendix) is also an experimentally observable quantity which has obvious significance for understanding the governing mechanism (including information about the nonperturbative effects). In our following tables we explicitly offer the theoretically estimated values for α corresponding to different mixing angles.

Using Eq. (8) we show the dependence of the ratio $\frac{\Gamma(\Xi_{cc}^{++} \rightarrow \Xi_c^+ \pi)}{\Gamma(\Xi_{cc}^{++} \rightarrow \Xi_c'^+ \pi)}$ on θ , which is depicted in Fig. 2 (the horizontal

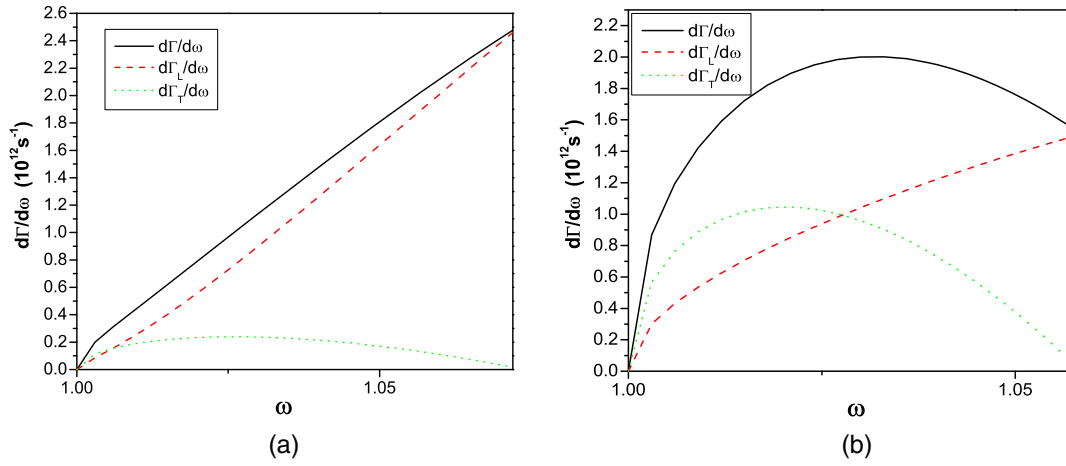


FIG. 3. Differential decay rates $d\Gamma/d\omega$ for the decay $\Xi_{cc}^{++} \rightarrow \Xi_c^+ l \bar{\nu}_l$ (a) and $\Xi_{cc}^{++} \rightarrow \Xi_c'^+ l \bar{\nu}_l$ (b) in [13] ($\theta = 0^\circ$).

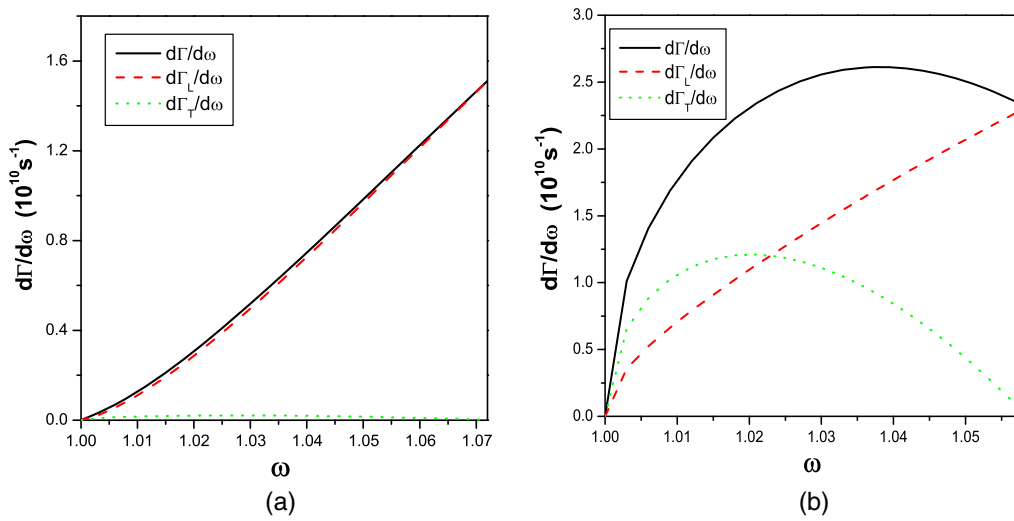


FIG. 4. Differential decay rates $d\Gamma/d\omega$ for the decay $\Xi_{cc}^{++} \rightarrow \Xi_c^+ l \bar{\nu}_l$ (a) and $\Xi_{cc}^{++} \rightarrow \Xi_c'^+ l \bar{\nu}_l$ (b) with $\theta = 16.27^\circ \pm 2.30^\circ$.

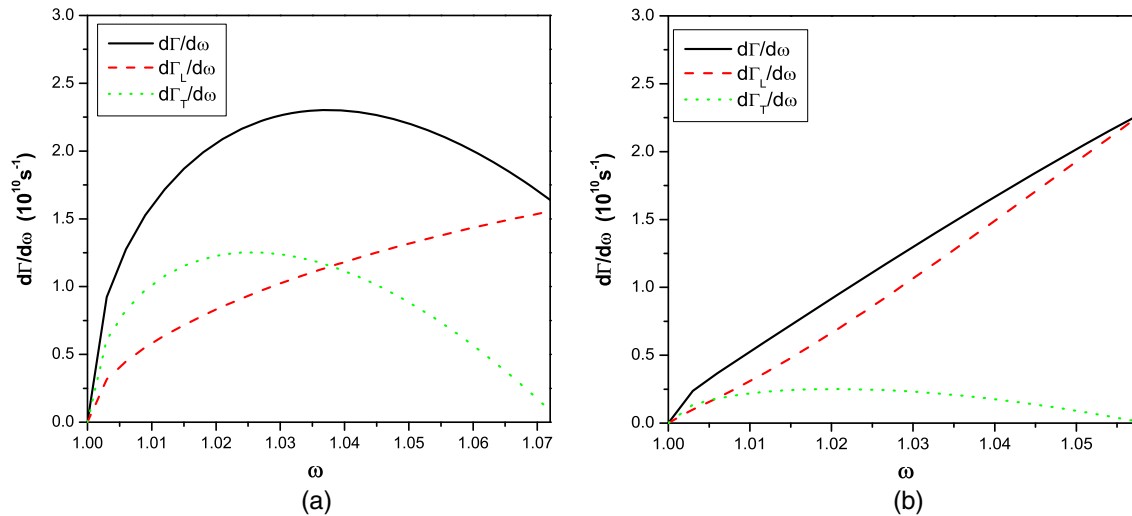


FIG. 5. Differential decay rates $d\Gamma/d\omega$ for the decay $\Xi_{cc}^{++} \rightarrow \Xi_c^+ l \bar{\nu}_l$ (a) and $\Xi_{cc}^{++} \rightarrow \Xi_c'^+ l \bar{\nu}_l$ (b) with $\theta = 85.54^\circ \pm 2.30^\circ$.

TABLE V. The width (in unit 10^{12} s^{-1}) and the ratio R of $\Xi_{cc}^{++} \rightarrow \Xi_c^+ \bar{\nu}_l$ (left) and $\Xi_{cc}^{++} \rightarrow \Xi_c'^+ \bar{\nu}_l$ (right).

	Γ	R	Γ	R
Results in [13] ($\theta = 0^\circ$)	0.100 ± 0.015	7.14 ± 0.61	0.0995 ± 0.0091	1.34 ± 0.07
$\theta = 16.27^\circ \pm 2.30^\circ$	0.0522 ± 0.0051	46.6 ± 0.5	0.130 ± 0.003	1.63 ± 0.05
$\theta = 85.54^\circ \pm 2.30^\circ$	0.143 ± 0.009	1.22 ± 0.04	0.0732 ± 0.0051	6.14 ± 0.57

band centered with the dotted line corresponds to the range allowed by the experimental error tolerance). With the data $1.41 \pm 0.17 \pm 0.10$ we fix θ to be $16.27^\circ \pm 2.30^\circ$ or $85.54^\circ \pm 2.30^\circ$. The mixing angle deviates from 0° , which might manifest the scale of the flavor SU(3) symmetry breaking for the concerned processes.

The mixing mechanism can change the predictions on the nonleptonic decays significantly. We list the estimated decay rates and up-down asymmetries of those processes with the three mixing angles in Tables II–IV. Comparing the results shown in the three tables, one can find

- (1) the orders of magnitude for the channels are unchanged with or without the mixing;
- (2) $\Xi_{cc}^{++} \rightarrow \Xi_c^{(\prime)+} \pi$ and $\Xi_{cc}^{++} \rightarrow \Xi_c^{(\prime)+} \rho$ are the main two-body decay channels for Ξ_{cc}^{++} ;
- (3) the relative sizes between $\Gamma(\Xi_{cc}^{++} \rightarrow \Xi_c^+ M)$ and $\Gamma(\Xi_{cc}^{++} \rightarrow \Xi_c'^+ M)$ are varied for the different mixing angles.

C. Semileptonic decays of $\Xi_{cc}^{++} \rightarrow \Xi_c^+ + \bar{\nu}_l$ and $\Xi_{cc}^{++} \rightarrow \Xi_c'^+ + \bar{\nu}_l$

Presetting different mixing angles, we repeat the evaluations of the rates of $\Xi_{cc}^{++} \rightarrow \Xi_c^+ \bar{\nu}_l$ and $\Xi_{cc}^{++} \rightarrow \Xi_c'^+ \bar{\nu}_l$. The dependence of the differential decay widths $d\Gamma/d\omega$ ($\omega = \frac{P \cdot P'}{mm'}$) on ω are depicted in Figs. 3–5. One can find that the curve shapes of Figs. 3 and 4 are similar for $\Xi_{cc}^{++} \rightarrow \Xi_c^+ \bar{\nu}_l$ and $\Xi_{cc}^{++} \rightarrow \Xi_c'^+ \bar{\nu}_l$. By contrast, the curve tendencies for $\Xi_{cc}^{++} \rightarrow \Xi_c^+ \bar{\nu}_l$ and $\Xi_{cc}^{++} \rightarrow \Xi_c'^+ \bar{\nu}_l$ in Figs. 3 and 5 are just left to right reversed from each other while the integrated quantities (decay widths) are close. The total decay widths and the ratio of the longitudinal to transverse decay rates R corresponding to the three mixing angles are all listed in Table V.

IV. CONCLUSIONS AND DISCUSSIONS

In Ref. [13] we calculated the transition rate of $\Xi_{cc}^{++} \rightarrow \Xi_c^{(\prime)+}$ in the light-front quark model with a three-quark picture of baryon. To calculate the transition $\Xi_{cc}^{++} \rightarrow \Xi_c^{(\prime)+}$ we need to know the inner spin-flavor structures of all the concerned baryons. Generally the two charm quarks constitute a diquark which joins the light quark to make the baryon Ξ_{cc}^{++} . Because two c quarks are identical heavy-flavor fermions in a color antitriplet, it must be a vector

boson. In Ref. [42] the scenario that light us pair in Ξ_c^+ ($\Xi_c'^+$) is preset as a scalar (vector) diquark was employed in our previous study [13]. With the prescription we calculate the form factors of the transition $\Xi_{cc}^{++} \rightarrow \Xi_c^{(\prime)+}$ and the decay rates of $\Xi_{cc}^{++} \rightarrow \Xi_c^{(\prime)+} \bar{\nu}_l$ and $\Xi_{cc}^{++} \rightarrow \Xi_c^{(\prime)+} M$.

However, we notice that the ratio $\Gamma(\Xi_{cc}^{++} \rightarrow \Xi_c^+ \pi)/\Gamma(\Xi_{cc}^{++} \rightarrow \Xi_c'^+ \pi)$ obtained with that prescription was 0.56 ± 0.18 [13], which does not agree with the data newly observed by the LHCb collaboration. To reconcile our theoretical result and data, we should find what was wrong and how to remedy the theoretical framework. One possible pitfall might be the spin-flavor structure of Ξ_c^+ ($\Xi_c'^+$) preset in Ref. [42], which was based on a precise SU(3) flavor symmetry. However, in fact the symmetry is upset by the difference between the mass of s quark and those of u and d quarks; to manifest this breaking we are motivated to suggest that the spin flavor of $[us]c$ in Ξ_c^+ ($\Xi_c'^+$) is the mixture of $[us]_0c$ and $[us]_1c$. By introducing a mixing angle θ the amplitudes become $\mathcal{A}(\Xi_{cc}^{++} \rightarrow \Xi_c^+) = \cos\theta \mathcal{A}([cc]_1[u] \rightarrow [us]_0[c]) + \sin\theta \mathcal{A}([cc]_1[u] \rightarrow [us]_1[c])$ and $\mathcal{A}(\Xi_{cc}^{++} \rightarrow \Xi_c'^+) = -\sin\theta \mathcal{A}([cc]_1[u] \rightarrow [us]_0[c]) + \cos\theta \mathcal{A}([cc]_1[u] \rightarrow [us]_1[c])$. Apparently the newly achieved ratio $\Gamma(\Xi_{cc}^{++} \rightarrow \Xi_c^+ \pi)/\Gamma(\Xi_{cc}^{++} \rightarrow \Xi_c'^+ \pi)$ depends on the parameter θ . We fix $\theta = 16.27^\circ \pm 2.30^\circ$ or $85.54^\circ \pm 2.30^\circ$ by fitting the data of LHCb.

Using the mixing angles we calculate the rates of semileptonic decays $\Xi_{cc}^{++} \rightarrow \Xi_c^+ \bar{\nu}_l$ and $\Xi_{cc}^{++} \rightarrow \Xi_c'^+ \bar{\nu}_l$. We find that the shapes of Figs. 3 and 4 are similar for $\Xi_{cc}^{++} \rightarrow \Xi_c^+ \bar{\nu}_l$ and $\Xi_{cc}^{++} \rightarrow \Xi_c'^+ \bar{\nu}_l$, respectively. By contrast, the curve tendencies for $\Xi_{cc}^{++} \rightarrow \Xi_c^+ \bar{\nu}_l$ and $\Xi_{cc}^{++} \rightarrow \Xi_c'^+ \bar{\nu}_l$ in Figs. 3 and 5 are just left to right reversed from each other. With the same theoretical framework, we also evaluate the rates of several nonleptonic decays. Our numerical results indicate that the order of magnitudes of these decays are unchanged but the relative sizes between $\Gamma(\Xi_{cc}^{++} \rightarrow \Xi_c^+ M)$ and $\Gamma(\Xi_{cc}^{++} \rightarrow \Xi_c'^+ M)$ are varied for the different mixing angles.

We hope that the experimentalists can make more precise measurements on those relevant decay channels of Ξ_{cc}^{++} . The new data would tell us whether our mechanism can survive; then, one can pin down the right one from the two possible mixing angles we fixed. Definitely, the theoretical studies on the double-heavy baryons would be helpful for getting a better understanding about the quark model and the nonperturbative QCD effects.

ACKNOWLEDGMENTS

This work is supported by the National Natural Science Foundation of China (NNSFC) under Contracts No. 12075167, No. 11735010, No. 12035009, and No. 12075125.

APPENDIX A: SEMILEPTONIC DECAYS OF $\mathcal{B}_1 \rightarrow \mathcal{B}_2 \bar{\nu}_l$

The helicity amplitudes are related to the form factors for $\mathcal{B}_1 \rightarrow \mathcal{B}_2 \bar{\nu}_l$ through the following expressions [43–45]:

$$\begin{aligned} H_{\frac{1}{2},0}^V &= \frac{\sqrt{Q_-}}{\sqrt{q^2}} \left((M_{\mathcal{B}_1} + M_{\mathcal{B}_2}) f_1 - \frac{q^2}{M_{\mathcal{B}_1}} f_2 \right), \\ H_{\frac{1}{2},1}^V &= \sqrt{2Q_-} \left(-f_1 + \frac{M_{\mathcal{B}_1} + M_{\mathcal{B}_2}}{M_{\mathcal{B}_1}} f_2 \right), \\ H_{\frac{1}{2},0}^A &= \frac{\sqrt{Q_+}}{\sqrt{q^2}} \left((M_{\mathcal{B}_1} - M_{\mathcal{B}_2}) g_1 + \frac{q^2}{M_{\mathcal{B}_1}} g_2 \right), \\ H_{\frac{1}{2},1}^A &= \sqrt{2Q_+} \left(-g_1 - \frac{M_{\mathcal{B}_1} - M_{\mathcal{B}_2}}{M_{\mathcal{B}_1}} g_2 \right), \end{aligned} \quad (\text{A1})$$

where $Q_{\pm} = 2(P \cdot P' \pm M_{\mathcal{B}_1} M_{\mathcal{B}_2})$ and $M_{\mathcal{B}_1} (M_{\mathcal{B}_2})$ represents $M_{\Xi_{cc}^{++}} (M_{\Xi_c^+})$. The amplitudes for the negative helicities are obtained in terms of the relation

$$H_{-\lambda' - \lambda_W}^{V,A} = \pm H_{\lambda' \lambda_W}^{V,A}, \quad (\text{A2})$$

where the upper (lower) index corresponds to $V(A)$. The helicity amplitudes are

$$H_{\lambda' \lambda_W} = H_{\lambda' \lambda_W}^V - H_{\lambda' \lambda_W}^A. \quad (\text{A3})$$

The helicities of the W -boson λ_W can be either 0 or 1, which correspond to the longitudinal and transverse polarizations, respectively. The longitudinally (L) and transversely (T) polarized rates are, respectively [43–45],

$$\begin{aligned} \frac{d\Gamma_L}{d\omega} &= \frac{G_F^2 |V_{cb}|^2 q^2 p_c M_{\mathcal{B}_2}}{(2\pi)^3 12M_{\mathcal{B}_1}} [|H_{\frac{1}{2},0}^V|^2 + |H_{-\frac{1}{2},0}^V|^2], \\ \frac{d\Gamma_T}{d\omega} &= \frac{G_F^2 |V_{cb}|^2 q^2 p_c M_{\mathcal{B}_2}}{(2\pi)^3 12M_{\mathcal{B}_1}} [|H_{\frac{1}{2},1}^V|^2 + |H_{-\frac{1}{2},-1}^V|^2], \end{aligned} \quad (\text{A4})$$

where p_c is the momentum of \mathcal{B}_2 in the rest frame of \mathcal{B}_1 .

The ratio of the longitudinal to transverse decay rates R is defined by

$$R = \frac{\Gamma_L}{\Gamma_T} = \frac{\int_1^{\omega_{\max}} d\omega q^2 p_c [|H_{\frac{1}{2},0}^V|^2 + |H_{-\frac{1}{2},0}^V|^2]}{\int_1^{\omega_{\max}} d\omega q^2 p_c [|H_{\frac{1}{2},1}^V|^2 + |H_{-\frac{1}{2},-1}^V|^2]}. \quad (\text{A5})$$

APPENDIX B: $\mathcal{B}_1 \rightarrow \mathcal{B}_2 M$

In general, the transition amplitude of $\mathcal{B}_1 \rightarrow \mathcal{B}_2 M$ can be written as

$$\begin{aligned} \mathcal{M}(\mathcal{B}_1 \rightarrow \mathcal{B}_2 P) &= \bar{u}_{\mathcal{B}_2} (A + B \gamma_5) u_{\mathcal{B}_1}, \\ \mathcal{M}(\mathcal{B}_1 \rightarrow \mathcal{B}_2 V) &= \bar{u}_{\mathcal{B}_2} \epsilon^{*\mu} [A_1 \gamma_\mu \gamma_5 + A_2 (p_c)_\mu \gamma_5 \\ &\quad + B_1 \gamma_\mu + B_2 (p_c)_\mu] u_{\mathcal{B}_1}, \end{aligned} \quad (\text{B1})$$

where ϵ^μ is the polarization vector of the final vector or axial-vector mesons. Including the effective Wilson coefficient $a_1 = c_1 + c_2/N_c$ (in Ref. [46] $a_1 = 1.05 \pm 0.10$), the decay amplitudes in the factorization approximation are [41]

$$\begin{aligned} A &= \lambda f_P (M_{\mathcal{B}_1} - M_{\mathcal{B}_2}) f_1(M^2), \\ B &= \lambda f_P (M_{\mathcal{B}_1} + M_{\mathcal{B}_2}) g_1(M^2), \\ A_1 &= -\lambda f_V M \left[g_1(M^2) + g_2(M^2) \frac{M_{\mathcal{B}_1} - M_{\mathcal{B}_2}}{M_{\mathcal{B}_1}} \right], \\ A_2 &= -2\lambda f_V M \frac{g_2(M^2)}{M_{\mathcal{B}_1}}, \\ B_1 &= \lambda f_V M \left[f_1(M^2) - f_2(M^2) \frac{M_{\mathcal{B}_1} + M_{\mathcal{B}_2}}{M_{\mathcal{B}_1}} \right], \\ B_2 &= 2\lambda f_V M \frac{f_2(M^2)}{M_{\mathcal{B}_1}}, \end{aligned} \quad (\text{B2})$$

where $\lambda = \frac{G_F}{\sqrt{2}} V_{cs} V_{q_1 q_2}^* a_1$ and M is the meson mass. Replacing P, V by S and A in the above expressions, one can easily obtain similar expressions for scalar and axial-vector mesons.

The decay rates of $\mathcal{B}_1 \rightarrow \mathcal{B}_2 P(S)$ and up-down asymmetries are [47]

$$\begin{aligned} \Gamma &= \frac{p_c}{8\pi} \left[\frac{(M_{\mathcal{B}_1} + M_{\mathcal{B}_2})^2 - M^2}{M_{\mathcal{B}_1}^2} |A|^2 \right. \\ &\quad \left. + \frac{(M_{\mathcal{B}_1} - M_{\mathcal{B}_2})^2 - m^2}{M_{\mathcal{B}_1}^2} |B|^2 \right], \\ \alpha &= -\frac{2\kappa \text{Re}(A^* B)}{|A|^2 + \kappa^2 |B|^2}, \end{aligned} \quad (\text{B3})$$

where p_c is the \mathcal{B}_2 momentum in the rest frame of \mathcal{B}_1 , m is the mass of pseudoscalar (scalar), and $\kappa = \frac{p_c}{M_{\mathcal{B}_2} + \sqrt{p_c^2 + M_{\mathcal{B}_2}^2}}$.

For $\mathcal{B}_1 \rightarrow \mathcal{B}_2 V(A)$ decays, the decay rate and up-down asymmetries are

$$\Gamma = \frac{p_c(E_{B_2} + M_{B_2})}{4\pi M_{B_1}} \left[2(|S|^2 + |P_2|^2) + \frac{\varepsilon^2}{m^2} (|S + D|^2 + |P_1|^2) \right],$$

$$\alpha = \frac{4m^2 \text{Re}(S^* P_2) + 2\varepsilon^2 \text{Re}(S + D)^* P_1}{2m^2 (|S|^2 + |P_2|^2) + \varepsilon^2 (|S + D|^2 + |P_1|^2)}, \quad (\text{B4})$$

where ε (m) is energy (mass) of the vector (axial vector) meson, and

$$S = -A_1,$$

$$P_1 = -\frac{p_c}{\varepsilon} \left(\frac{M_{B_1} + M_{B_2}}{E_{B_2} + M_{B_2}} B_1 + M_{B_1} B_2 \right),$$

$$P_2 = \frac{p_c}{E_{B_2} + M_{B_2}} B_1,$$

$$D = -\frac{p_c^2}{\varepsilon(E_{B_2} + M_{B_2})} (A_1 - M_{B_1} A_2). \quad (\text{B5})$$

-
- [1] R. Aaij *et al.* (LHCb Collaboration), *Phys. Rev. Lett.* **119**, 112001 (2017).
- [2] R. Aaij *et al.* (LHCb Collaboration), *Phys. Rev. Lett.* **121**, 162002 (2018).
- [3] R. Aaij *et al.* (LHCb Collaboration), [arXiv:2202.05648](https://arxiv.org/abs/2202.05648).
- [4] W. Wang, F. S. Yu, and Z. X. Zhao, *Eur. Phys. J. C* **77**, 781 (2017).
- [5] Y. J. Shi, W. Wang, and Z. X. Zhao, *Eur. Phys. J. C* **80**, 568 (2020).
- [6] N. Sharma and R. Dhir, *Phys. Rev. D* **96**, 113006 (2017).
- [7] A. S. Gerasimov and A. V. Luchinsky, *Phys. Rev. D* **100**, 073015 (2019).
- [8] H. Y. Cheng, G. Meng, F. Xu, and J. Zou, *Phys. Rev. D* **101**, 034034 (2020).
- [9] T. Gutsche, M. A. Ivanov, J. G. Körner, V. E. Lyubovitskij, and Z. Tyulemissov, *Phys. Rev. D* **99**, 056013 (2019).
- [10] T. Gutsche, M. A. Ivanov, J. G. Körner, and V. E. Lyubovitskij, *Phys. Rev. D* **96**, 054013 (2017).
- [11] T. Gutsche, M. A. Ivanov, J. G. Körner, V. E. Lyubovitskij, and Z. Tyulemissov, *Phys. Rev. D* **100**, 114037 (2019).
- [12] M. A. Ivanov, J. G. Körner, and V. E. Lyubovitskij, *Phys. Part. Nucl.* **51**, 678 (2020).
- [13] H. W. Ke, X. H. Liu, and X. Q. Li, *Eur. Phys. J. C* **82**, 144 (2022).
- [14] W. Jaus, *Phys. Rev. D* **41**, 3394 (1990); **44**, 2851 (1991); **60**, 054026 (1999).
- [15] C. R. Ji, P. L. Chung, and S. R. Cotanch, *Phys. Rev. D* **45**, 4214 (1992).
- [16] H. Y. Cheng, C. Y. Cheung, and C. W. Hwang, *Phys. Rev. D* **55**, 1559 (1997).
- [17] H. Y. Cheng, C. K. Chua, and C. W. Hwang, *Phys. Rev. D* **69**, 074025 (2004).
- [18] C. D. Lü, W. Wang, and Z. T. Wei, *Phys. Rev. D* **76**, 014013 (2007).
- [19] H. M. Choi, *Phys. Rev. D* **75**, 073016 (2007).
- [20] H. W. Ke, X. Q. Li, and Z. T. Wei, *Phys. Rev. D* **80**, 074030 (2009).
- [21] H. W. Ke, X. Q. Li, Z. T. Wei, and X. Liu, *Phys. Rev. D* **82**, 034023 (2010).
- [22] G. Li, F. I. Shao, and W. Wang, *Phys. Rev. D* **82**, 094031 (2010).
- [23] H. W. Ke, X. Q. Li, and Z. T. Wei, *Eur. Phys. J. C* **69**, 133 (2010).
- [24] H. W. Ke, X. H. Yuan, and X. Q. Li, *Int. J. Mod. Phys. A* **26**, 4731 (2011).
- [25] H. W. Ke and X. Q. Li, *Phys. Rev. D* **84**, 114026 (2011).
- [26] H. W. Ke and X. Q. Li, *Eur. Phys. J. C* **71**, 1776 (2011).
- [27] Z. T. Wei, H. W. Ke, and X. Q. Li, *Phys. Rev. D* **80**, 094016 (2009).
- [28] H. W. Ke, N. Hao, and X. Q. Li, *J. Phys. G* **46**, 115003 (2019).
- [29] H. W. Ke, N. Hao, and X. Q. Li, *Eur. Phys. J. C* **79**, 540 (2019).
- [30] F. S. Yu, H. Y. Jiang, R. H. Li, C. D. Lü, W. Wang, and Z. X. Zhao, *Chin. Phys. C* **42**, 051001 (2018).
- [31] C. K. Chua, *Phys. Rev. D* **99**, 014023 (2019).
- [32] H. Y. Cheng and C. K. Chua, *J. High Energy Phys.* **11** (2004) 072.
- [33] H. Y. Cheng, C. K. Chua, and C. W. Hwang, *Phys. Rev. D* **70**, 034007 (2004).
- [34] H. W. Ke, X. Q. Li, and Z. T. Wei, *Phys. Rev. D* **77**, 014020 (2008).
- [35] H. W. Ke, X. H. Yuan, X. Q. Li, Z. T. Wei, and Y. X. Zhang, *Phys. Rev. D* **86**, 114005 (2012).
- [36] S. Tawfiq, P. J. O'Donnell, and J. G. Körner, *Phys. Rev. D* **58**, 054010 (1998).
- [37] Q. Chang, X. N. Li, X. Q. Li, F. Su, and Y. D. Yang, *Phys. Rev. D* **98**, 114018 (2018).
- [38] C. Q. Geng, C. W. Liu, Z. Y. Wei, and J. Zhang, *Phys. Rev. D* **105**, 073007 (2022).

- [39] A. F. Falk, M. E. Luke, M. J. Savage, and M. B. Wise, *Phys. Rev. D* **49**, 555 (1994).
- [40] C. H. Chang, T. Li, X. Q. Li, and Y. M. Wang, *Commun. Theor. Phys.* **49**, 993 (2008).
- [41] J. G. Körner and M. Kramer, *Z. Phys. C* **55**, 659 (1992).
- [42] D. Ebert, R. N. Faustov, and V. O. Galkin, *Phys. Rev. D* **73**, 094002 (2006).
- [43] J. G. Körner and M. Kramer, *Phys. Lett. B* **275**, 495 (1992).
- [44] P. Bialas, J. G. Körner, M. Kramer, and K. Zalewski, *Z. Phys. C* **57**, 115 (1993).
- [45] J. G. Körner, M. Kramer, and D. Pirjol, *Prog. Part. Nucl. Phys.* **33**, 787 (1994).
- [46] A. J. Buras, *Nucl. Phys.* **B434**, 606 (1995).
- [47] H. Y. Cheng, *Phys. Rev. D* **56**, 2799 (1997).